

This article was published in

Seppälä A, Lampinen MJ. 1999. Thermodynamic optimizing of pressure-retarded osmosis power generation systems. *Journal of Membrane Science* 161: 115-138.

© 1999 Elsevier Science

Reprinted with permission.



ELSEVIER

Journal of Membrane Science 161 (1999) 115–138

Journal of
MEMBRANE
SCIENCE

Thermodynamic optimizing of pressure-retarded osmosis power generation systems

Ari Seppälä*, Markku J. Lampinen

*Helsinki University of Technology, Department of Energy Engineering, Laboratory of Applied Thermodynamics,
P.O. Box 4100, FIN-02015 HUT, Finland*

Received 4 January 1999; received in revised form 2 March 1999; accepted 4 March 1999

Abstract

A transport equation for a solution flow increasing due to osmosis inside a hollow cylindrical fibre is derived. The equation can be applied for either direct, pressure-retarded or reverse osmosis, when the membrane is highly selective. This transport equation is used to study theoretically the net power delivered, and the entropy generated by two different concepts of a pressure-retarded osmosis power production system. As a result, the system can be optimized either by maximizing the net power or maximizing the ratio (Ψ) between the net power and entropy generation. In both cases the optimal values of the initial hydrostatic pressure difference between the inner and the outer sides of the fibre, the initial velocity of the solution and the fibre length could be specified. However, in some cases these two methods of optimization result in remarkably different optimal values. The resulting net power, when Ψ was maximized, was found to drop to less than half the maximum net power. The local entropy generation was found always to result in a minimum value at a certain longitudinal position inside the fibre. © 1999 Elsevier Science B.V. All rights reserved.

Keywords: Osmosis; Transport equation; Power and entropy generation; Thermodynamics

1. Introduction

In a pressure-retarded osmosis power generating system river water and salty sea water (brine) are directed to different sections of an osmotic unit. The flows are separated from each other by semi-permeable membranes. Due to osmosis, the river water penetrates through the membranes and mixes with the pressurized brine. The membrane can be thought of as an energy converter between the osmotic power (caused by the salinity gradient) and the hydro-

static pressure. In theory, the concentration difference between the sea- and river water could be a considerable energy source: an osmotic pressure of 20 bar, which refers to a salt concentration of about 830 mol/m³ (or 24 g salt/kg water) can be thought of as a hydrostatic pressure head corresponding to a 204 m high waterfall. Although our system of interest deals with sea- and river-water, a similar system could exist in principle for any other solution–membrane system for which the solute is highly impermeable and where fresh water is obtainable.

Earlier studies [1–5] on the pressure retarded osmosis system for power generation mostly concern

*Corresponding author. E-mail: ari.seppala@hut.fi

experimental and economic subjects or consider the transport of the permeating flow through the membrane wall. None of the earlier works, as far as we know, include the transport equation for the brine flow where changes in the hydrostatic pressure, brine concentration and volume flow are included. This is essential when we want to predict the possible output values of an osmotic unit. The volume flow of the brine, the concentration and the hydrostatic pressure are all interrelated, so disregarding the changes in one of them might cause an important cross-related phenomenon to be neglected.

For energy production, the brine must be pressurized to result in any net power. Furthermore, the osmotic pressure difference ($\Delta\pi$) between the two sides of the membrane must be higher than the hydrostatic pressure difference (Δp) to induce the increasing brine flow, and thus to result in net power. Therefore, we assume, there will be an optimum value of Δp somewhere between the upper ($\Delta p < \Delta\pi$) and the lower ($\Delta p > 0$) limits, which results in maximum power generation. The purpose of this paper is to locate theoretically the actual optimal point and also to study whether there are similar optimum points in respect of other system parameters such as initial mean velocity, fibre radius and fibre length. In addition, we examine how the quality of the energy conversion process in the form of the entropy generation can be applied to the optimization. Readers who are not interested in the entropy analysis may skip Section 4 and Sections 5.6 and 5.7 and still get full information concerning the derivation and behaviour of the transport equation and the results of optimizing the net power.

2. The concept of pressure-retarded osmosis for power production

The pressure-retarded osmosis power generation system (Fig. 1) contains

1. a pump which pumps the needed brine flow at the needed hydrostatic pressure.
2. an osmotic unit which consists of numerous thin hollow cylindrical fibres. The walls of the fibres are considered as semi-permeable membranes. The brine is directed to flow inside the hollow fibres and the freshwater outside the fibres. Due to the

lower chemical potential inside a hollow fibre than on the outside, the fresh water permeates through the semi-permeable surface to the brine. So, the brine flow increases and dilutes. In pressure retarded osmosis the brine is pressurized, retarding the permeating flow. The hydrostatic pressure drops in the unit. The membrane has to be highly selective i.e. the flow of solute through the membrane should be minimal. If the hydrostatic pressure of the brine exceeds or the osmotic pressure drops below a certain value, the water will flow from the brine to the fresh water side (reverse osmosis) and if the hydrostatic pressure is equal on both sides, the fresh water will permeate through the semi-permeable walls to the brine due only to the osmotic pressure (direct osmosis).

3. the fresh water side. The fresh water is directed to flow outside the fibres and it may also need some pumping but in general the pressure loss will be considerably lower than on the brine side.
4. a turbine which transforms the momentum of the brine flow into work.

The components 1–4 form the basic concept of osmotic power generation system (BS). Furthermore, an improved system (IS) was studied (first presented in [6]). The improvement to the BS (see the system inside the dashed line in Fig. 1) involves the addition of two brine tanks and another water pump to move the brine from the ocean to the tank without pressurizing it. While one tank is filled with new brine from the ocean, the brine from the other tank is pumped to flow through the osmotic unit and an equal volume flow is directed to return to the same tank. Thus, in the IS the flow through the turbine equals the permeating flow. The unused brine in the tank and the recycled, diluted brine are separated from each other in the tank by an impermeable membrane. Instead of using the pump for pressurizing the brine, the returned brine pressurizes the tank and the power demand of the pump drops. When the tank is full of recycled brine, the other tank which, meanwhile is filled with brine from the ocean, is connected to establish flow through the osmotic unit.

The power demand of the pump is $\dot{V}_{\text{pump}}\Delta p_{\text{pump}}/\eta_{\text{pump}}$ and the power delivered by the turbine is $\eta_{\text{turb}}\dot{V}_{\text{turb}}\Delta p_{\text{turb}}$, where η is the efficiency, \dot{V} the volume flow and Δp the pressure change. The hydrostatic pressure changes are regarded as negligible

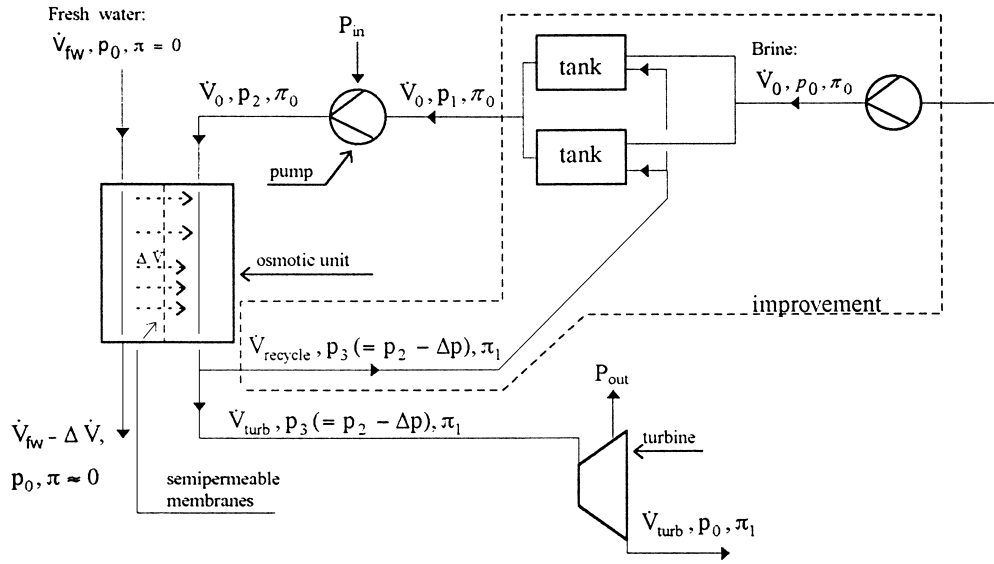


Fig. 1. The pressure-retarded osmotic power generation scheme. The system inside the dashed line is an improvement from the basic concept. Different osmotic pressures (π) of flows are consequences of corresponding salt concentration of the brine.

everywhere except at the brine side of the osmotic unit, at the pump (in IS the power of the pump that moves the brine from the ocean to the tank is negligible too) and at the turbine. Using the notations of Fig. 1

for BS:

$$\dot{V}_{\text{recycle}} = 0, \quad \dot{V}_{\text{turb}} = \dot{V}_0 + \Delta\dot{V}, \quad p_1 = p_0$$

and for IS:

$$\dot{V}_{\text{recycle}} = \dot{V}_0, \quad \dot{V}_{\text{turb}} = \Delta\dot{V}, \quad p_1 = p_3$$

The net power obtained from the BS is then

$$P_{\text{BS}} = \eta_{\text{turb}}(\dot{V}_0 + \Delta\dot{V})(p_3 - p_0) - \frac{\dot{V}_0(p_2 - p_0)}{\eta_{\text{pump}}} \quad (1a)$$

and from the IS

$$P_{\text{IS}} = \eta_{\text{turb}}\Delta\dot{V}(p_3 - p_0) - \frac{\dot{V}_0(p_2 - p_3)}{\eta_{\text{pump}}} \quad (1b)$$

If $\eta_{\text{turb}} = \eta_{\text{pump}} = 1$, we get $P_{\text{BS}} = P_{\text{IS}}$. Eqs. (1a) and (1b) may be carried forward into a form

$$P_{\text{BS}} = \eta_{\text{turb}}\dot{V}_{z=L}\Delta p_{z=L} - \left[\frac{\dot{V}_{z=0}\Delta p_{z=0}}{\eta_{\text{pump}}} \right] \quad (2a)$$

$$P_{\text{IS}} = \eta_{\text{turb}}[\dot{V}_{z=L} - \dot{V}_{z=0}]\Delta p_{z=L} - \left[\frac{\dot{V}_{z=0}[\Delta p_{z=0} - \Delta p_{z=L}]}{\eta_{\text{pump}}} \right] \quad (2b)$$

where $\Delta p_{z=0}$ and $\Delta p_{z=L}$ are the hydrostatic pressure differences over the membrane at the beginning ($z=0$) and at the end ($z=L$) of the osmotic unit, respectively. For the permeating volume flux per surface area of a membrane, we use the equation derived according to the linear theory of irreversible thermodynamics [7]. The equation can be written in a local form

$$\dot{V}_{\text{perm}}''(z) = L_{\text{filt}}[L_{\text{refl}}\Delta\pi(z) - \Delta p(z)] \quad (3)$$

where $\Delta p(z) (=p(z) - p_0)$ and $\Delta\pi(z)$ are, respectively, the hydrostatic pressure difference and the osmotic pressure difference at a longitudinal position z between the brine at the inner surface of the fibre and the fresh water at the outer surface of the fibre. The reflection coefficient L_{refl} depends on both the properties of the membrane and solute. If $L_{\text{refl}} = 1$, the membrane is fully semi-permeable i.e. all the solute is 'reflected' from the membrane, otherwise $L_{\text{refl}} < 1$. L_{filt} is the filtration coefficient of the membrane. Although for power generation we need highly impermeable membranes where the salt flux is almost zero

($L_{\text{refl}} \approx 1$), significant salt polarization inside the porous side of an asymmetric fibre may occur even under minute solute flow through the membrane. For this kind of case Loeb and Mehta [2] presented a two-coefficient equation and Lee et al. [5] a three-coefficient equation, the additive coefficient being a measure of the resistance to salt transport in the porous substrate. Both these equations (for [5] with an assumption that on the fresh water side the solute concentration is zero) and Eq. (3) as well, may be cast into a form $\dot{V}_{\text{perm}}'' = A \Delta\pi - B \Delta p$ where A and B are the coefficients. However, Loeb and Mehta and Lee et al. found that the coefficient A may get (for asymmetric membranes with porous substructure) remarkably lower values than the product of the coefficients L_{filt} and L_{refl} in Eq. (3). For this reason we shall interpret the coefficient L_{refl} more freely than is normally done. All the results in Section 5 are calculated using an effective osmotic pressure difference $\Delta\pi_{\text{eff}} = L_{\text{refl}} \Delta\pi$ where for L_{refl} can thus be assigned remarkably lower values than unity even with minimal solute flux. Loeb [8] has studied also effect of porous support fabric of Loeb–Sourirajan type membranes.

An extremely simplified model for maximum net power and optimal hydrostatic pressure difference Δp_{opt} can be derived if the pressure loss inside the osmotic unit, the dilution of the solution ($\Delta\pi(z) = \text{constant}$) and the efficiency ($\eta_{\text{turb}} = \eta_{\text{pump}} = 1$) is neglected. As now $\Delta\dot{V} = (\dot{V}_{\text{perm}}'')(A_{\text{membrane surface}})$ the net power is achieved by combining Eqs. (1a), (1b) and (3). The optimal pressure difference corresponding to the maximum net power is achieved from the zero point of the derivative of the net power. The result is

$$\Delta p_{\text{opt}} = \frac{L_{\text{refl}} \Delta\pi}{2} \quad \text{and} \quad \frac{P_{\text{maximum}}}{A_{\text{membrane surface}}} = \frac{L_{\text{filt}} (L_{\text{refl}} \Delta\pi)^2}{4}$$

Thus, in the case of a fully semi-permeable membrane surface the optimum hydrostatic pressure difference would be half of the osmotic pressure difference.

3. Transport equation for a brine flow increasing due to osmosis inside a hollow cylindrical fibre

3.1. Derivation of the transport equation

The equation of continuity for a component i in a flow of solution inside a hollow cylindrical fibre can be

set as a convection–diffusion problem in a stationary state:

$$\nabla \cdot \mathbf{n}_i = 0 \quad (4)$$

where \mathbf{n}_i is the mass flux of species i relative to stationary coordinates

$$\mathbf{n}_i = \rho_i \mathbf{v} + \mathbf{j}_i \quad (5)$$

where \mathbf{v} is mass average velocity vector of a solution and the diffusion flux

$$\mathbf{j}_i = -\rho D \nabla \left(\frac{\rho_i}{\rho} \right) \quad (6)$$

We assume that in the z direction (longitudinal direction of the fibre) the diffusion flux is meaningless compared to the convective flow ($\rho_i v_z$). At the surface of the membrane (highly selective) and at the centre of the fibre (symmetry line) the salt-flux in the radial r direction $n_{s,r} \approx 0$. Assuming this is applicable everywhere in radial direction leads to the mass average velocity in radial direction

$$v_r = \frac{\rho D}{\rho_s} \frac{\partial}{\partial r} \left(\frac{\rho_s}{\rho} \right).$$

Under the above assumptions, when divided by the molar mass of salt, the continuity Eq. (4) results for salt in

$$v_z \frac{\partial c_s}{\partial z} + c_s \frac{\partial v_z}{\partial z} = 0 \quad (7)$$

We continue to assume that the velocity in the z direction achieves separated solutions i.e.

$$v_z(r, z) = F(r)G(z) \quad (8)$$

where $F(r)$ and $G(z)$ are some yet unknown functions. Inserting this into Eq. (7) we get

$$G(z) \frac{\partial c_s(r, z)}{\partial z} + c_s(r, z) \frac{dG(z)}{dz} = 0 \quad (9)$$

the solution of which is

$$c_s = \frac{f(r)}{G(z)} \quad (10)$$

i.e. also salt concentration satisfies a separated solution of form $c_s(r, z) = f(r)g(z)$ where $g(z) = (1/G(z))$ and $f(r)$ is some yet unknown function.

At the entrance the flow is assumed to satisfy the profile of laminar fully developed flow

$$v_z(r, z = 0) = 2v_{\text{mean}}^0 \left[1 - \left(\frac{r}{r_0} \right)^2 \right] \quad (11)$$

where v_{mean}^0 is the initial mean velocity. For the initial salt concentration we set a condition

$$c_s(r = r_0, z = 0) = \text{constant} = c_s^0 \quad (12)$$

As the permeating flow (Eq. (3)) must be equal to the change of the brine flow, the boundary condition at the surface can be written (when $\rho_{\text{water, fresh}} \approx \rho_{\text{brine}}$) as

$$\begin{aligned} L_{\text{filt}} [L_{\text{refl}} \Delta \pi(r = r_0, z) - \Delta p(r = r_0, z)] \\ = \frac{1}{2\pi r_0} \frac{\partial}{\partial z} \left(\int_0^{r_0} v_z(r, z) dA \right) \end{aligned} \quad (13)$$

where the differential cross-sectional area $dA = 2\pi r dr$. For a dilute solution the osmotic potential may be written as

$$\Delta \pi = RTc_s \quad (14)$$

Applying the boundary condition Eq. (11) to Eq. (8) we set

$$G(z = 0) = 2v_{\text{mean}}^0 \quad (15a)$$

$$F(r) = 1 - \left(\frac{r}{r_0} \right)^2 \quad (15b)$$

Inserting Eq. (15b) into Eq. (8) and substituting the result into Eq. (13), results after solving the integral and applying Eqs. (10) and (14) in the form

$$L_{\text{filt}} \left[\frac{L_{\text{refl}} RT f(r = r_0)}{G(z)} - \Delta p(z) \right] = \frac{r_0}{4} \frac{dG(z)}{dz} \quad (16)$$

The constant value of $f(r = r_0)$ can be obtained from the boundary condition Eq. (12)

$$c_s^0 = \frac{f(r = r_0)}{G(z = 0)} = \frac{f(r = r_0)}{2v_{\text{mean}}^0} \Rightarrow f(r = r_0) = 2v_{\text{mean}}^0 c_s^0 \quad (17)$$

Substituting this into Eq. (16), we get

$$\frac{dG(z)}{dz} = \frac{A_1}{G(z)} + A_2 \Delta p(z) \quad (18)$$

where the constants A_1 and A_2 are

$$A_1 = \frac{8L_{\text{filt}}L_{\text{refl}}RTv_{\text{mean}}^0 c_s^0}{r_0}, \quad A_2 = -\frac{4L_{\text{filt}}}{r_0}$$

Eq. (18) may be solved analytically in two cases. First, when the hydrostatic pressure difference $\Delta p(z, r = r_0) \approx 0$ (direct osmosis) results in applying also Eq. (15a) to the solution

$$G = \sqrt{2A_1 z + 4(v_{\text{mean}}^0)^2}$$

and the velocity in the z direction is thus

$$v_z(r, z) = \left(1 - \left(\frac{r}{r_0} \right)^2 \right) \sqrt{2A_1 z + 4(v_{\text{mean}}^0)^2}.$$

Integrating over the cross-sectional area of the fibre we get for the mean volume flow

$$\dot{V}_{\text{mean}} = \pi r_0^2 \sqrt{\frac{A_1 z}{2} + (v_{\text{mean}}^0)^2}$$

This equation might be usable in other cases but here it means that the power generation of the system vanishes (see Eqs. (2a) and (2b) when $\Delta p(z) = 0$).

In the second case, if the pressure difference function is a multiplied function of the function $G(z)$ and some other function $\Omega(z)$ (i.e. $\Delta p(z) = G(z)\Omega(z)$), Eq. (18) returns to the non-linear ordinary differential Bernoulli equation of first order which can be in some cases solved by changing variables. However, this yielded complicated results for the function G even with simple equations of the function $\Omega(z)$, such as $\Omega(z) = bz$ or $\Omega(z) = e^{bz}$, where b is a constant, and there is no guarantee that such analytical results can satisfy any real velocity profiles or pressure difference functions. Therefore, we choose a different approach which results in numerical integration of the transport equation.

The pressure drop of the brine flow is solved from the z -component of the Navier–Stokes equation of motion for an incompressible fluid with constant viscosity (μ) in radial coordinates:

$$\rho \frac{dv_z}{dt} = F_z - \frac{\partial p}{\partial z} + \mu \left[\frac{\partial^2 v_z}{\partial r^2} + \frac{1}{r} \frac{\partial v_z}{\partial r} + \frac{1}{r^2} \frac{\partial^2 v_z}{\partial \theta^2} + \frac{\partial^2 v_z}{\partial z^2} \right] \quad (19)$$

For symmetry ($\partial^2 v_z / \partial \theta^2 = 0$) and the acceleration term (the left-hand side of Eq. (19)) and the external

force F_z terms can be considered as meaningless. We are interested in the pressure at the surface where, due to the friction, also $v_z = 0$. With the above statements and when substituting Eqs. (8) and (15b) into Eq. (19), this results in

$$\left(\frac{\partial p}{\partial z}\right)_{r=r_0} = \frac{-4\mu G(z)}{r_0^2} \quad (20)$$

which yields after integration

$$p(z) = p(z=0) - \frac{4\mu}{r_0^2} \int_0^z G(z) dz \quad (21)$$

After this is substituted into Eq. (18) we get

$$\frac{dG(z)}{dz} = \frac{A_1}{G(z)} + A_2 \left[\Delta p^0 - A_3 \int_0^z G(z) dz \right] \quad (22)$$

where $A_3 = (4\mu/r_0^2)$ and $\Delta p^0 = p(z=0) - p_0$. Eq. (22) may be written equivalently in the form

$$\frac{dG(z)}{dz} = \frac{A_1}{G(z)} + A_2 \left[\Delta p(z_1) - A_3 \int_{z_1}^z G(z) dz \right] \quad (23)$$

The numerical integration of Eq. (23) is carried through using the following procedure

$$\begin{cases} G^n = G^{n-1} + \left\{ \frac{A_1}{G^{n-1}} + A_2 \Delta p^n \right\} \Delta z \\ \Delta p^n = \Delta p^{n-1} - A_3 G^{n-1} \Delta z \end{cases} \quad (24)$$

Each time a new value of G^n is solved from Eq. (24), the corresponding volume flow is evaluated from

$$\dot{V}^n = \int_0^{r_0} G^n F(r) dA = \frac{r_0^2 G^n}{4}$$

and the net power from Eqs. (2a) and (2b) can be written in the form

$$P_{BS}^n = \eta_{\text{turb}} \dot{V}^n \Delta p^n - \frac{\dot{V}^0 \Delta p^0}{\eta_{\text{pump}}} \quad (25a)$$

$$P_{IS}^n = \eta_{\text{turb}} (\dot{V}^n - \dot{V}^0) \Delta p^n - \frac{\dot{V}^0 (\Delta p^0 - \Delta p^n)}{\eta_{\text{pump}}} \quad (25b)$$

Eq. (23) takes into account the concentration boundary layer of the flow of the solution in the radial direction also. However, here it is necessary to solve the solute concentration only on the surface. The

possible solute boundary layer inside the wall of an asymmetric fibre (internal polarization) is taken into account with the reflectivity coefficient as mentioned in Section 2.

3.2. The mechanism controlling osmotic growth of the brine flow

The level where the brine flow inside a hollow fibre settles is controlled by two different mechanisms which are coupled together. The physical connections between velocities, pressures and concentrations are illustrated in Fig. 2. First, if the brine flow is decreased e.g. due to the increased initial hydrostatic pressure (increase from an arbitrary reference value of p_{ref}) or due to the decreased (from an arbitrary reference value $v_{\text{mean,ref}}^0$) initial mean velocity, the pressure losses will settle at a lower level. This, in turn, results in higher $p(z_1)$ (or equivalently $\Delta p(z_1)$) than if we had started with the lower values of p_{ref} or $v_{\text{mean,ref}}^0$ and consequently lowers the level of the permeating flow, thus causing the brine flow to decrease further. Correspondingly, if the brine flow increases, this mechanism causes a self-exciting effect in the brine flow.

The rate of change of brine flow (or permeating flow) also has a contradictory self-regulating mechanism: when brine flow decreases, the salt concentration settles at a higher level and consequently causes the permeating flow to grow and thus the brine flow to grow as well (then the increased brine flow can influence again either by diminishing or augmenting itself). So, if the brine flow increases, this effect can prohibit the growth to a certain extent and if the brine flow decreases, this mechanism can prevent the brine flow from ceasing.

4. Derivation of the entropy generation function

The second law of thermodynamics for a closed system in the general form of Clausius–Duhem inequality is

$$S(B) - S(A) \geq \int_A^B \frac{dQ}{T} \quad (26)$$

where S is the entropy of the system, T the absolute temperature, A is the initial state of the system and B

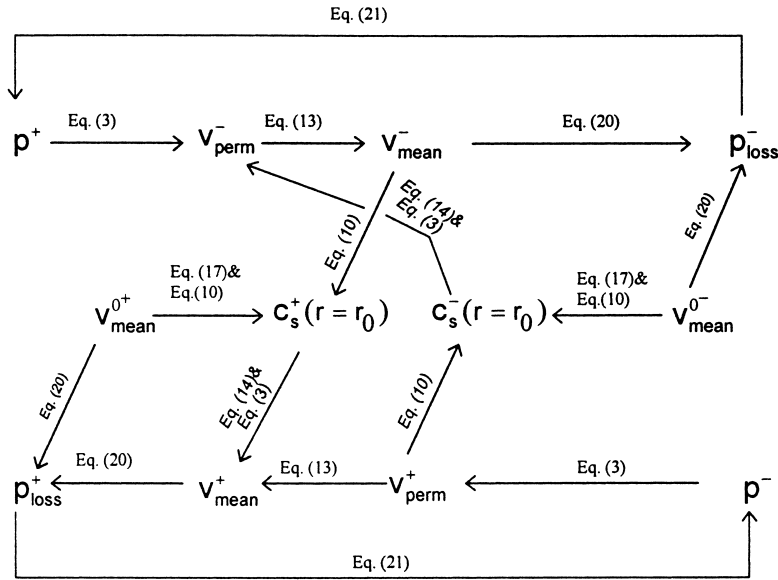


Fig. 2. The connection mechanism between changes of hydrostatic pressure (p), permeating flow (v_{perm}), initial mean brine flow (v_{mean}^0), mean brine flow (v_{mean}), pressure losses of brine (p_{loss}) and salt concentration of the brine on the inner surface of the fibre ($C_s(r = r_0)$). The (+) sign means increase (from an arbitrary reference value) of the parameter and the (-) sign decrease (from an arbitrary reference value) of the parameter. The hydrostatic pressure (p) can also be interpreted as the initial hydrostatic pressure or as the hydrostatic pressure difference across the membrane. The equation numbers correspond to those that give rise to the cause-and-effect connection.

the state of the system after the transformation process. The equality sign indicates a reversible process. Eq. (26) can also be written as

$$S(B) - S(A) = \int_A^B \frac{dQ}{T} + S_{gen} \quad (27)$$

where S_{gen} is the entropy generation inside the system. Comparing Eqs. (26) and (27) we see that always $S_{gen} \geq 0$ and thus for irreversible processes inside the system (such as heat conduction, chemical reactions, mixing of species and mass flow) $S_{gen} > 0$ and for reversible processes $S_{gen} = 0$.

For a stationary flow system Eq. (27) can be derived further into the form

$$\sum_{out} Ns - \sum_{in} Ns = \sum_n \frac{\dot{Q}_n}{T_n} + \sigma \quad (28)$$

where the left-hand side comprises the entropy flow due to mass flows (s is the specific entropy and N the molar flux) and the term $\sum_n (\dot{Q}_n/T_n)$ is the entropy flow due to the heat flow \dot{Q}_n at temperature level T_n . As the system stays in a stationary state, the entropy of the

system remains constant. The entropy produced inside the system (at rate $\sigma \geq 0$) flows outside the system thus increasing the entropy of the environment. The irreversibilities of the system of Fig. 1 are assumed to be generated in the osmotic unit. The entropy generation in the pump and turbine will be meaningful only if the efficiency is extremely low. The control system (the osmotic unit or a part of it) for the entropy analysis is shown in Fig. 3. The system is assumed to remain isothermal.

The molar specific entropy of species i in an ideal solution can be written in the form

$$s_i(T, p, x_i) = s_i^0(T) - v_i \gamma_i (p - p_0) - R \ln x_i \quad (29)$$

where x is the mole fraction, R the universal gas constant, $s^0(T)$ the reference entropy at a temperature T (the temperature of the system) and reference pressure p_0 which equals the pressure of the fresh water, v the partial molar volume and γ the isobaric coefficient of volume expansion. We assume that the pressure on the brine side does not vary significantly in the radial direction so that the calculated pressure at the surface can be applied everywhere in r direction. Thus, as the pressure on the fresh water side is set to the reference

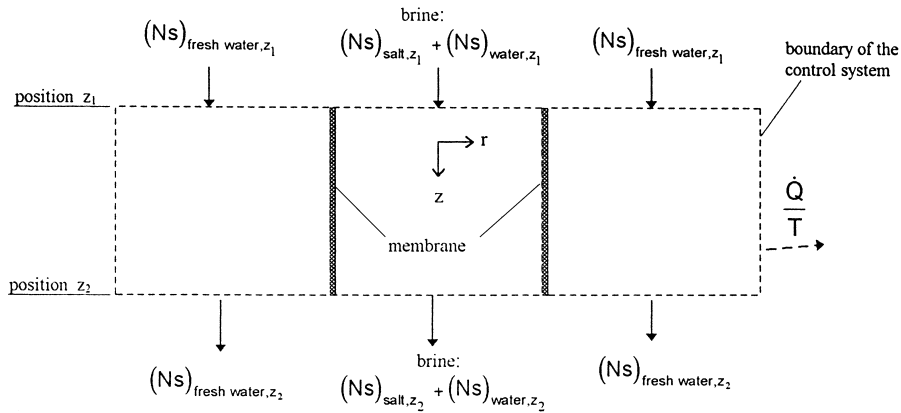


Fig. 3. The control system for the entropy analysis. The flows of entropy are indicated with arrows. The position z_1 and z_2 are arbitrary, so that the control system could be interpreted as any macroscopic longitudinal section of the osmotic unit, or as the whole unit as well.

pressure p_0 and as the pressure loss on the fresh water side was assumed in Section 2 to be negligible, the pressure difference in Eq. (29) is $p(z) - p_0 = \Delta p(z)$. The $\Delta p(z)$ is calculated from Eq. (24).

The entropy flow due to the mass flow inside the fibre at level z can be solved by integrating the product of the velocity, specific entropy and concentration profiles over the cross-sectional area of the fibre and summing the salt and water components

$$(Ns)_{\text{brine},z} = \int_0^{r_0} s_s(r,z)c_s(r,z)v_z(r,z) dA + \int_0^{r_0} s_w(r,z)c_w(r,z)v_z(r,z) dA \quad (30)$$

As the pressure drop on the fresh water side is negligible, as the system remains isothermal and as the salt flux through the membrane is negligible, the specific entropy on the fresh water side remains constant. Thus, the change of entropy flowterm for the fresh water is

$$(Ns)_{\text{fw},z_2} - (Ns)_{\text{fw},z_1} = -\Delta \dot{V} c_{\text{fw}}^0 s_{\text{fw}}^0(T) \quad (31)$$

where the decrease of the volume flow is equal to the rise of the volume flow on the brine side. The change in volume flow can be solved from

$$\Delta \dot{V} = \int_0^{r_0} v_z(r,z_2) dA - \int_0^{r_0} v_z(r,z_1) dA \quad (32)$$

Inserting the cross-sectional area $dA = 2\pi r dr$ and Eqs. (8) and (15b) into the above and performing the integration results in

$$\Delta \dot{V} = \frac{\pi r_0^2}{2} [G(z_2) - G(z_1)] \quad (33)$$

As the brine is considered in this study as a dilute solution, we simplify the integration of Eq. (30) assuming that the concentration and mole fraction of the water in the brine are constants $c_w = c_w^0 = c_{\text{fw}}$ and $x_w = c_w^0 / (c_w^0 + c_s^0)$, respectively. Still, an additional assumption has to be made because the concentration distribution in the radial direction was left unsolved: we assume that the initial profile at the inlet of the osmotic unit $c_s(r,z=0) \approx c_s^0$. So, applying Eq. (10) and the relation $G(z=0) = 2v_{\text{mean}}^0$ we get a constant value for the function $f(r) = f = 2v_{\text{mean}}^0 c_s^0$. Thus, the mole fraction of salt yields

$$x_s(z) = \frac{2v_{\text{mean}}^0 c_s^0 / G(z)}{2v_{\text{mean}}^0 c_s^0 / G(z) + c_w^0} \quad (34)$$

The integration of Eq. (30) can now be completed by applying the relations from Eqs. (8), (10), (15b) and (29). Summing all the entropy flows, caused by mass flows, results in the form

$$\begin{aligned} \sum_{\text{out}} Ns - \sum_{\text{in}} Ns = & A_5 \ln \left[\frac{c_w^0 G(z_2) + 2c_s^0 v_{\text{mean}}^0}{c_w^0 G(z_1) + 2c_s^0 v_{\text{mean}}^0} \right] \\ & - A_6 [G(z_2) - G(z_1)] \\ & - A_7 [\Delta p(z_2)G(z_2) - \Delta p(z_1)G(z_1)] \end{aligned} \quad (35)$$

where the reference entropies have disappeared. The constants are

$$A_5 = 2Rc_s^0 v_{\text{mean}}^0 A_g, \quad A_6 = R \ln x_w^0 c_w^0 A_8,$$

$$A_7 = \gamma_w v_w c_w^0 A_8, \quad A_8 = \frac{\pi r_0^2}{2},$$

We have excluded the $\gamma_s v_s c_s \Delta p$ term for salt as it is considered small compared to the respective term for water.

For the osmotic unit to remain isothermal, there must be a heat flow through system boundaries balancing the generating dissipation heat. The heat flow can be solved by setting an energy balance for the osmotic unit

$$\sum_{\text{out}} Nh - \sum_{\text{in}} Nh = \dot{Q} \quad (36)$$

where h is the molar specific enthalpy. The change of the kinetic energy is ignored as it is considered small compared to the heat flow and to the change of enthalpy. The total derivative of the specific enthalpy of a single component can be written for an isothermal process

$$dh_i = v_i(1 - T\gamma_i) dp \quad (37)$$

Assuming v and γ to be independent of pressure, and assuming bulk properties for the brine, the heat flow can be solved from the energy balance

$$\dot{Q} = [\dot{V}(z_2) \Delta p(z_2) - \dot{V}(z_1) \Delta p(z_1)](1 - T\gamma_w) \quad (38)$$

where $\Delta p(z) = p(z) - p_0$.

Inserting Eqs. (35) and (38) into Eq. (28) results in the final equation for the rate of entropy generation between levels z_1 and z_2 .

$$\sigma = A_5 \ln \left[\frac{c_w^0 G(z_2) + 2c_s^0 v_{\text{mean}}^0}{c_w^0 G(z_1) + 2c_s^0 v_{\text{mean}}^0} \right]$$

$$- A_6 [G(z_2) - G(z_1)] - [A_7 + A_9] [\Delta p(z_2) G(z_2) - \Delta p(z_1) G(z_1)] \quad (39)$$

where $A_9 = [(1 - \gamma_w T)/T] A_8$. The $\Delta p(z)$ and $G(z)$ values are calculated from Eq. (24). We define the rate of local entropy generation as

$$\sigma''' = \frac{\sigma}{A_{\text{fibre}} \Delta z} \quad (40)$$

where A_{fibre} is the cross-sectional area of the fibre,

$\Delta z = z_2 - z_1$ is such a small difference of z that diminishing Δz would not change the result with the needed accuracy. In practice the same value of Δz is used here as in Eq. (24). We shall use the rate of the entropy generation, not only directly in the form of Eqs. (39) and (40) but also as a function

$$\Psi = \frac{P}{\sigma} \quad (41)$$

and

$$\varepsilon = \frac{P}{P + \sigma T} \quad (42)$$

Eq. (41) could be interpreted as the ratio of the power produced by the system to the thermodynamical impact on the environment. In Eq. (42) the same idea is described in a different form. The dimensionless energy conversion efficiency results in a maximum value, unity, when the entropy generation vanishes. T is given the system temperature value. As the system is assumed to remain isothermal, T equals the temperature of brine at the inlet i.e. the temperature of the ocean.

5. Results and discussion

5.1. The effect of changing Δp^0 only

First we examine the effect of changing the initial hydrostatic pressure difference Δp^0 between the inner and outer surfaces of the fibre. We can interpret this also as changing the initial hydrostatic pressure on the brine side as the pressure on the outer side is assumed to remain constant. At first we keep other parameters constant: the effective initial osmotic pressure difference $\Delta \pi_{\text{eff}}^0 = 25$ bar ($\pi_{\text{eff}}^0 = L_{\text{ref}} RT c_s^0$, L_{ref} may take into account also the possible internal polarization, see comments in Section 2), the fibre radius $r_0 = 50$ μm , $\mu = 0.000855$ N s/m², $\eta_{\text{turb}} = 0.9$, $\eta_{\text{pump}} = 0.8$, $L_{\text{filt}} = 10^{-11}$ m/s Pa and the initial mean velocity $v_{\text{mean}}^0 = 0.08$ m/s were used. The results of calculation are shown in Fig. 4. After a rapid increase, the mean velocity settles at a lower growth rate due to the dilution of brine i.e. due to the lowered osmotic pressure. Due to the higher pressure drop, i.e. higher hydrostatic pressure difference across the membrane, the growth of velocity stays at a higher level with

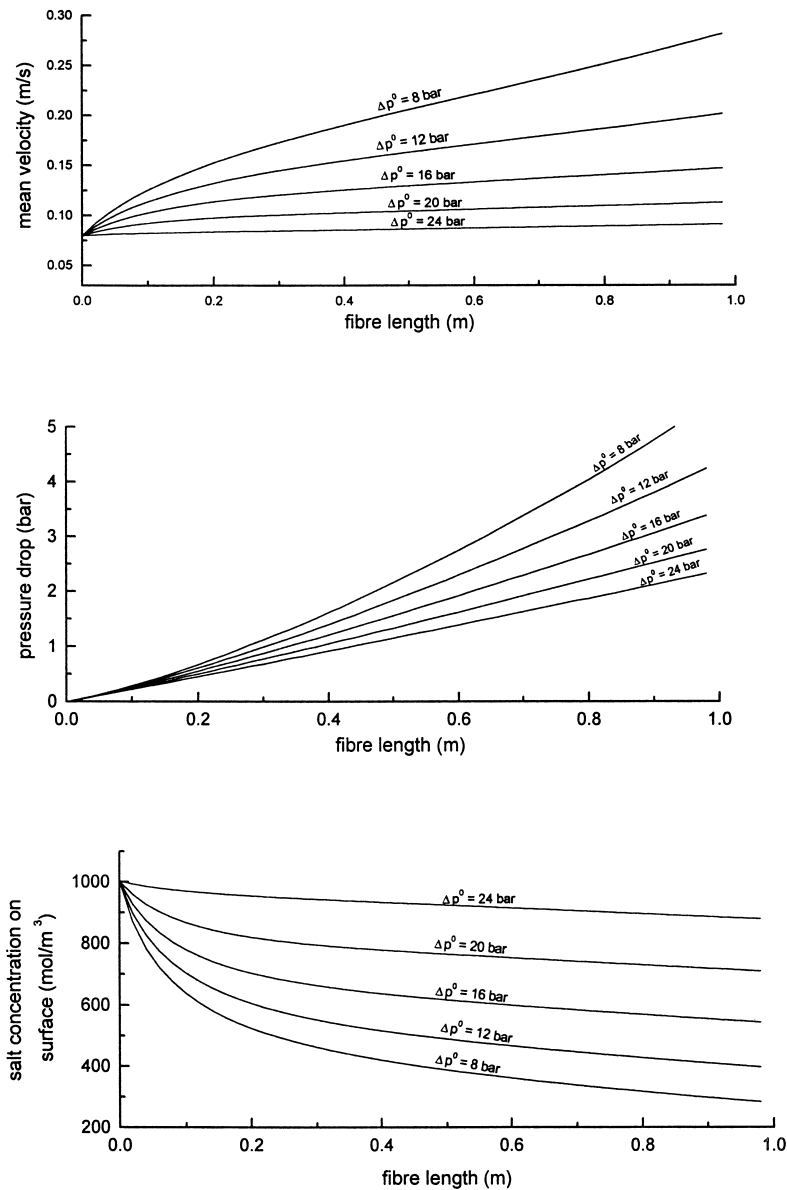


Fig. 4. The effect of the initial hydrostatic pressure difference on (a) the mean velocity of brine; (b) the hydrostatic pressure drop inside the fibre and (c) salt concentration on the inner surface of the fibre. The following constant values were used for all figures: $L_{\text{fil}} = 10^{-11}$ m/s Pa, $\Delta\pi_{\text{eff}}^0 = 25$ bar, $r_0 = 50$ μm , $v_{\text{mean}}^0 = 0.08$ m/s, $\mu = 0.000855$ N s/m².

higher v_{mean}^0 . As a consequence of the results of the pressure and velocity, the net power Eq. (25a) of the BS always gives a maximum value at some specific z position (Fig. 5). Furthermore, we see that there might possibly also be an optimal value of Δp^0 as the values

8 bar and 12 bar give higher net power than the values below 8 bar and the values over 12 bar. From Fig. 5, we also find that the positive net power can be achieved only with a certain combination of Δp^0 and fibre length (L). Similar phenomena results also

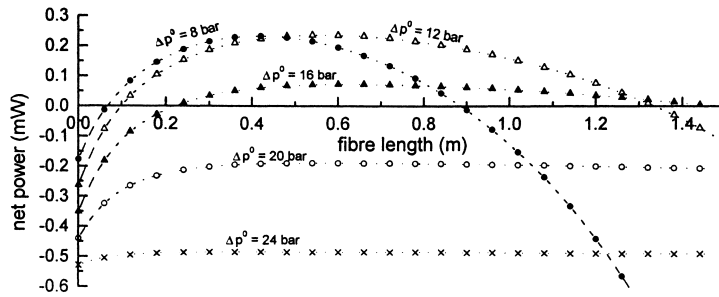


Fig. 5. The effect of the initial hydrostatic pressure difference on the resulting net power of BS corresponding to Fig. 4. The efficiencies used were $\eta_{\text{turb}} = 0.9$, $\eta_{\text{pump}} = 0.8$.

when the net power Eq. (25b) of the improved system is applied.

5.2. The effect of changing v_{mean}^0 only

The results (see Fig. 6) when v_{mean}^0 is changed while the other initial values are kept constant give rather similar behaviour for the pressure drop and velocity profiles to when only Δp^0 was changed. Constant values $\Delta\pi_{\text{eff}}^0 = 25$ bar, $r_0 = 50$ μm , $\mu = 0.000855$ N s/m², $\eta_{\text{turb}} = 0.9$, $\eta_{\text{pump}} = 0.8$, $L_{\text{filt}} = 10^{-11}$ m/s Pa, $\Delta p_0 = 12$ bar were used. In this case the concentration profiles show a different kind of behaviour: at first, the salt concentration results in higher values the higher the value of v_{mean}^0 is. However, after certain fibre length, the order is the opposite, so that the highest v_{mean}^0 results in the lowest concentrations, and the lowest velocities in the highest concentrations. This can be explained by the fact that although the highest v_{mean}^0 (i.e. the highest volume flow of salt as well) results in the highest salt concentration at the beginning of the fibre, it also causes the highest increase of the velocity i.e. highest permeating of the fresh water and so the dilution is highest. The net power Eq. (25a) of BS gives, as it did also when only Δp^0 was changed, a maximum value at some specific position in the longitudinal direction. From Fig. 7 it can be seen that there might again occur an optimal value as the velocities 0.05 and 0.08 m/s give higher net power than the velocities below 0.05 m/s and the velocities over 0.08 m/s. The positive net power is also in this case achieved only with a certain combination of v_{mean}^0 and L . Similar phenomena results too when using net power Eq. (25b) of the IS.

5.3. The maximization of the net power—the optimal values of Δp^0 , v_{mean}^0 and L

As was found in Sections 5.1 and 5.2 a maximum point exists for the net power in respect of L for each value of v_{mean}^0 and Δp^0 we have studied the consequence of changing both v_{mean}^0 and Δp^0 . Results with the values $\Delta\pi_{\text{eff}}^0 = 25$ bar and $r_0 = 50$ μm are illustrated in Figs. 8 and 9. In these figures each point corresponds to a maximum power delivered by the BS in respect to the fibre length. In Fig. 8 can be seen the positive range (white area) of the net power surrounded by the non-power generating $v_{\text{mean}}^0 - \Delta p^0$ parameter space. In Fig. 9 the parameter space resulting in the positive net power generation has been zoomed. The corresponding optimal fibre lengths (L_{opt}) are illustrated in Fig. 10. By increasing the calculated $v_{\text{mean}}^0 - \Delta p^0$ density, an optimal parameter pair $v_{\text{mean,opt-P}}^0 - \Delta p_{\text{opt-P}}^0$ which results in the highest net power generation, can be found at the needed accuracy. The optimized maximum net power P_{maximum} of the case of Figs. 8, 9 and 10 is 0.274 mW at $v_{\text{mean,opt-P}}^0 = 0.059$ m/s, $\Delta p_{\text{opt-P}}^0 = 9.53$ bar and $L_{\text{opt-P}} = 0.55$ m.

5.4. The maximum power with different initial effective osmotic pressures, fibre radii and efficiency

So far, we have shown the existence of the maximum power generation P_{maximum} which corresponds to the optimum parameters $v_{\text{mean,opt-P}}^0$ and $\Delta p_{\text{opt-P}}^0$, $L_{\text{opt-P}}$. Here we shall study what happens to $v_{\text{mean,opt-P}}^0$, $\Delta p_{\text{opt-P}}^0$, $L_{\text{opt-P}}$ and P_{maximum} when $\Delta\pi_{\text{eff}}^0$, r_0 , η_{pump} and η_{turb} are changed while the rest

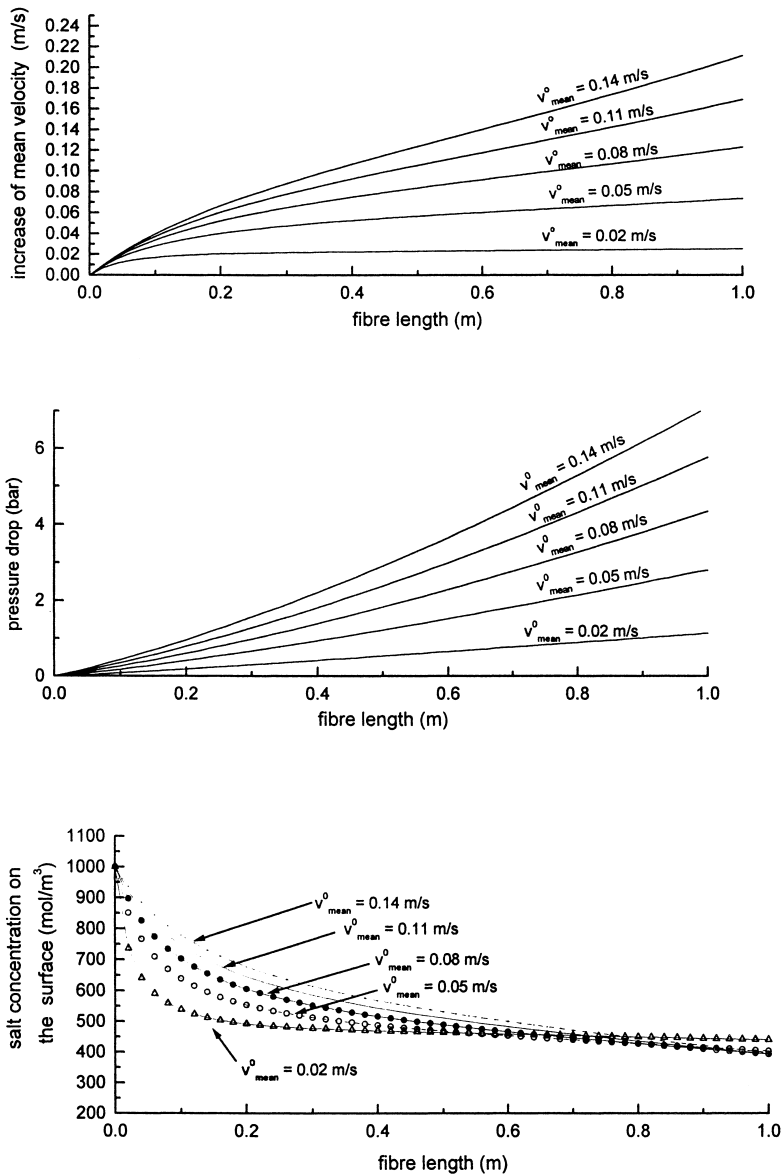


Fig. 6. The effect of the initial hydrostatic pressure difference on (a) the mean velocity of brine, ($= v_{\text{mean}}(z) - v_{\text{mean}}^0$); (b) the hydrostatic pressure drop inside the fibre and (c) salt concentration on the inner surface of the fibre. The following constant values were used for all figures: $L_{\text{filt}} = 10^{-11}$ m/s Pa, $\Delta\pi_{\text{eff}}^0 = 25$ bar, $r_0 = 50$ μm , $\Delta p^0 = 12$ bar, $\mu = 0.000855$ N s/m².

of the parameters L_{filt} and μ are kept constant. Changing $\Delta\pi_{\text{eff}}^0$ could be interpreted in such a way that any of the parameters L_{ref} , T or c_s^0 could be changed while some or other parameters are kept constant. However, for c_s^0 it should be noted that Eq. (14) holds for a dilute, ideal solution and for the viscosity that it depends on T and the mixture composition. According

to the results in Figs. 11 and 12 and Tables 1–3 we conclude the following:

1. $v_{\text{mean,opt-P}}^0$ values grow almost linearly with increasing $\Delta\pi_{\text{eff}}^0$.
2. $\Delta p_{\text{opt-P}}^0$ values are independent of the fibre radius.
3. $\Delta p_{\text{opt-P}}^0$ is almost linearly dependent on $\Delta\pi_{\text{eff}}^0$.
4. $L_{\text{opt-P}}$ is independent of the $\Delta\pi_{\text{eff}}^0$.

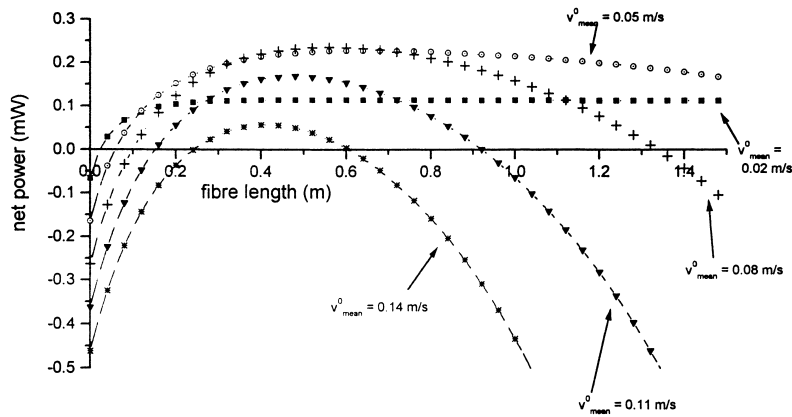


Fig. 7. The effect of the initial mean velocity on the resulting net power of BS corresponding to Fig. 6. The efficiencies used were $\eta_{\text{turb}} = 0.9$, $\eta_{\text{pump}} = 0.8$.

5. The ratio between P_{maximum} and the surface area of the fibre (corresponding to the $L_{\text{opt-P}}$) increases when $\Delta\pi_{\text{eff}}^0$ increases but remains independent of r_0 .
6. The power density (P_{maximum} divided by the fibre volume corresponding to the $L_{\text{opt-P}}$) increases when $\Delta\pi_{\text{eff}}^0$ increases but decreases when r_0 increases.
7. IS results in higher P_{maximum} values than the BS (in real systems where the efficiency is lower than unity). The more the efficiency of the pump and the

turbine deviate from the unity, the bigger becomes the difference between the IS and the BS P_{maximum} values. The simplified model for maximum power given in the end of Section 2, where the pressure loss, dilution of solution and the pump and turbine efficiency are neglected, results in remarkably overestimated values.

8. The ratio between initial volume flow and total permeating flow ($\dot{V}_0/\Delta\dot{V}$) is independent on r_0 and on $\Delta\pi_{\text{eff}}^0$. For the BS the ratio depends strongly on

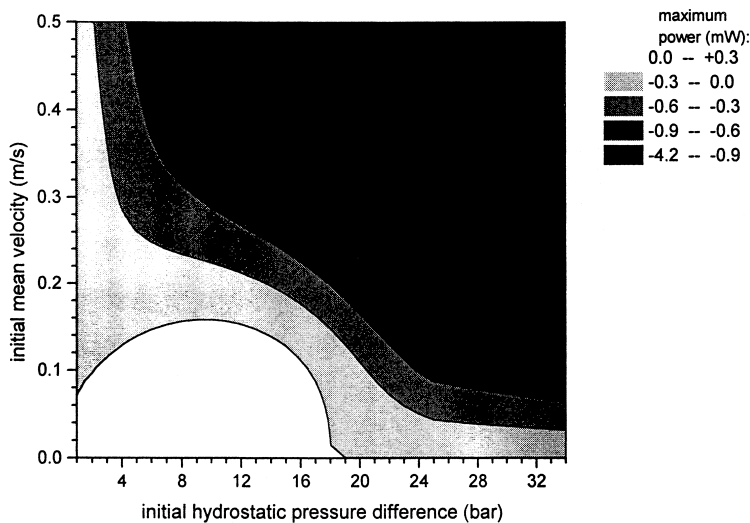


Fig. 8. The maximum power (BS) as a function of the initial pressure difference and the initial mean velocity of brine. Constant values $\Delta\pi_{\text{eff}}^0 = 25$ bar, $L_{\text{filt}} = 10^{-11}$ m/s Pa, $r_0 = 50$ μm , $\mu = 0.000855$ N s/m², $\eta_{\text{turb}} = 0.9$, $\eta_{\text{pump}} = 0.8$ were used. Each point on the map corresponds to the maximum power delivered by the system in respect of the fibre length.

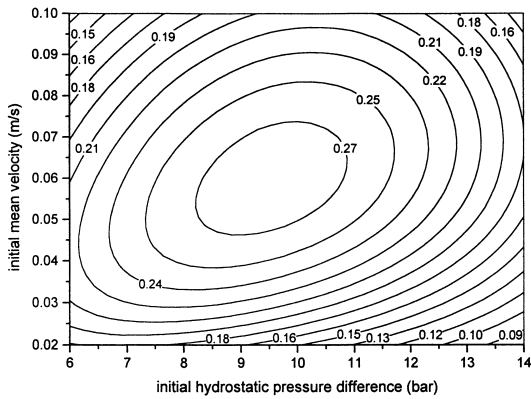


Fig. 9. The positive maximum power (mW) range of Fig. 8. Each point on the map corresponds to the maximum power delivered by the system in respect of the fibre length. The corresponding fibre lengths are shown at Fig. 10.

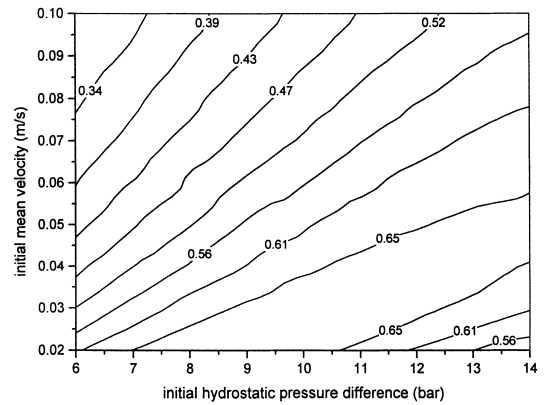


Fig. 10. The optimum fibre length corresponding to Figs. 8 and 9.

the efficiency but for the IS the dependency is weak. For the IS this ratio can also be interpreted as a ratio between the recycled flow and the flow passing through the turbine.

Here it should be noted that although Δp_{opt-P}^0 is independent of the fibre radius, it is valid only when the correct values of L_{opt-P} and $v_{mean,opt-P}^0$ (which

depend on the radius) are used. If, for instance, the fibre length is fixed as some arbitrary value, the Δp_{opt-P}^0 does not result in $P_{maximum}$ (see e.g. Fig. 5). All above conclusions hold for both BS and IS.

In reference [5] the permeating water flux was evaluated by the three coefficient equation mentioned in Section 2 of this article. The coefficients were reached by direct and reverse osmosis measurements

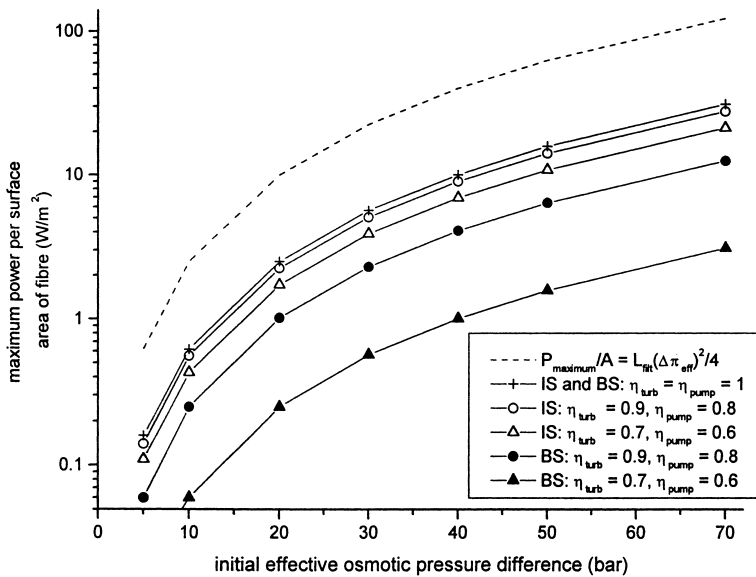


Fig. 11. The maximum power divided by the surface area of the fibre. The ratio becomes independent of the radius of the fibre. The dashed curve corresponds to power ($=L_{fit}\Delta\pi_{eff}^2/4$) when pressure loss, dilution of the solution and the efficiencies are neglected (the simplified model is presented in Section 2). The following constant parameter values were used: $L_{fit} = 10^{-11}$ m/s Pa, $\mu = 0.000855$ N s/m².

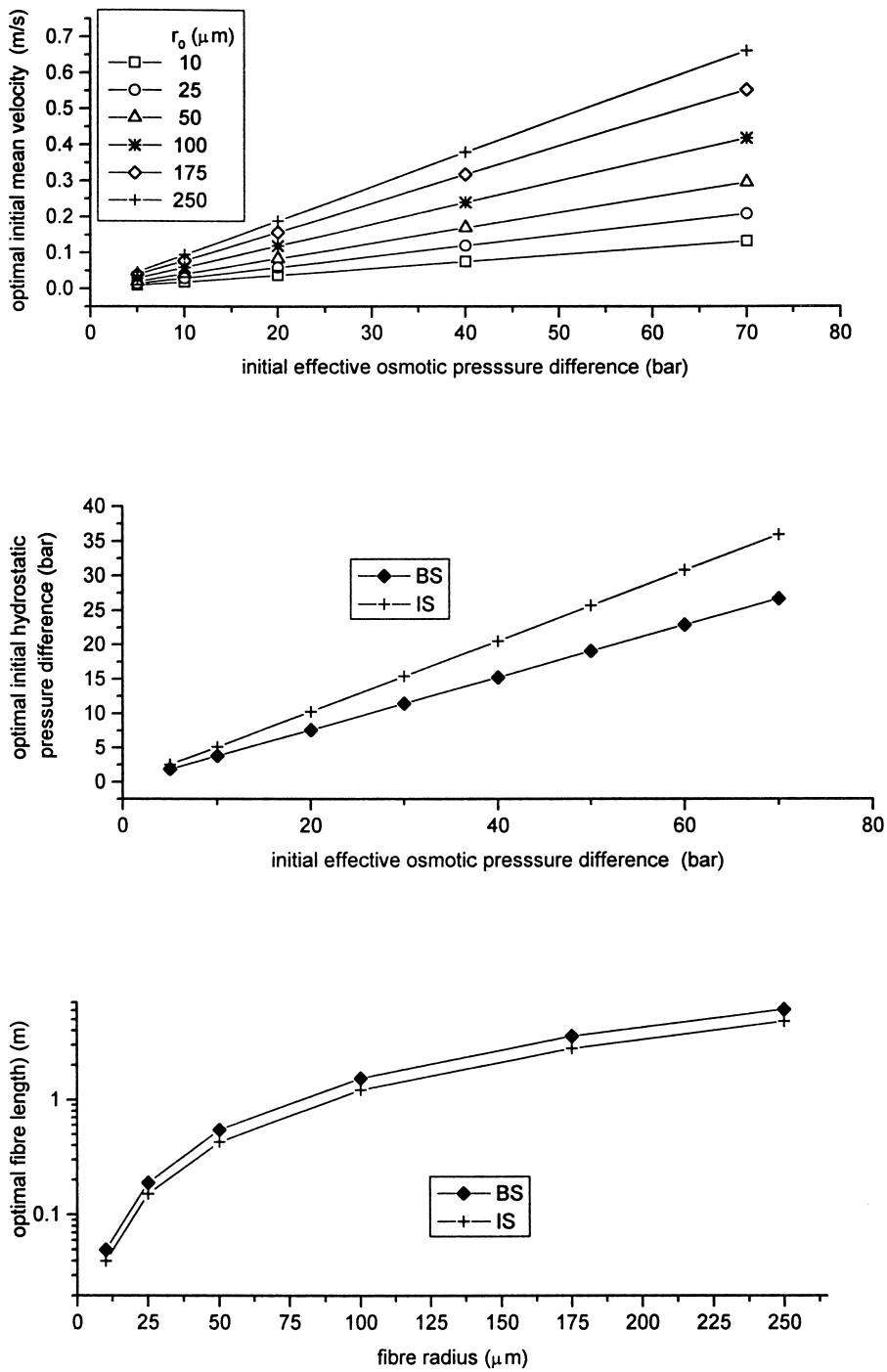


Fig. 12. The optimal (a) initial mean velocity of brine for the IS; (b) initial hydrostatic pressure difference (same for all fibre radii) for IS and BS; (c) fibre length (same for all osmotic pressures) of IS and BS. Constant values $L_{fill} = 10^{-11}$ m/s Pa, $\mu = 0.000855$ N s/m², $\eta_{urb} = 0.9$, $\eta_{pump} = 0.8$ were used.

Table 1

The maximum power density ($\text{kW}/\text{m}^3_{\text{fibre}}$) of BS with the different effective osmotic pressures and fibre radii

| $\Delta\pi_{\text{eff}}^0$ (bar) | $r_0 = 10 \mu\text{m}$ | $r_0 = 25 \mu\text{m}$ | $r_0 = 50 \mu\text{m}$ | $r_0 = 100 \mu\text{m}$ | $r_0 = 175 \mu\text{m}$ | $r_0 = 250 \mu\text{m}$ |
|----------------------------------|------------------------|------------------------|------------------------|-------------------------|-------------------------|-------------------------|
| 5 | 13 | 4.8 | 2.5 | 1.3 | 0.7 | 0.5 |
| 10 | 51 | 21 | 10 | 5.1 | 2.9 | 2.0 |
| 20 | 197 | 83 | 41 | 20 | 12 | 8.1 |
| 40 | 802 | 333 | 162 | 81 | 46 | 33 |
| 70 | 2461 | 1018 | 497 | 250 | 142 | 100 |

The constants: $L_{\text{filt}} = 10^{-11} \text{ m/s Pa}$, $\mu = 0.000855 \text{ N s/m}^2$, $\eta_{\text{turb}} = 0.9$, $\eta_{\text{pump}} = 0.8$.

Table 2

The maximum power density ($\text{kW}/\text{m}^3_{\text{fibre}}$) of S with the different effective osmotic pressures and fibre radii

| $\Delta\pi_{\text{eff}}^0$ (bar) | $r_0 = 10\mu\text{m}$ | $r_0 = 25 \mu\text{m}$ | $r_0 = 50 \mu\text{m}$ | $r_0 = 100\mu\text{m}$ | $r_0 = 175 \mu\text{m}$ | $r_0 = 250 \mu\text{m}$ |
|----------------------------------|-----------------------|------------------------|------------------------|------------------------|-------------------------|-------------------------|
| 5 | 24 | 11 | 5.6 | 2.8 | 1.6 | 1.1 |
| 10 | 108 | 45 | 22 | 11 | 6.4 | 4.5 |
| 20 | 430 | 180 | 90 | 45 | 26 | 18 |
| 40 | 1735 | 720 | 360 | 179 | 103 | 72 |
| 70 | 5308 | 2206 | 1103 | 550 | 315 | 220 |

The constants: $L_{\text{filt}} = 10^{-11} \text{ m/s Pa}$, $\mu = 0.000855 \text{ N s/m}^2$, $\eta_{\text{turb}} = 0.9$, $\eta_{\text{pump}} = 0.8$.

with asymmetric and composite flat sheet membranes. The resulting net power of a system corresponding to the BS of this article was then calculated neglecting the pressure losses, dilution of the solution and the pump and turbine efficiency. The best results corresponded the net power calculated by the simplified model of this article (see e.g. Fig. 11).

According to the results, the smaller the inner radius of the fibre is, the higher power density the system delivers. However, the usefulness of thin fibres is restricted by the need for short optimum length, which causes the other system dimensions to expand; as the fibre radius decreases, e.g. the demand of the number of fibres increases causing a possible increase in losses at inlet and outlet of fibres.

Table 3

The ratio between initial volume flow and total permeating flow ($\dot{V}_0/\Delta\dot{V}$) for BS and IS with different efficiencies. The ratio is independent of the fibre radius and on the initial osmotic pressure

| | $\eta_{\text{turb}}=0.7$ $\eta_{\text{pump}} = 0.6$ | $\eta_{\text{turb}} = 0.8$ $\eta_{\text{pump}} = 0.7$ | $\eta_{\text{turb}} = 0.9$ $\eta_{\text{pump}} = 0.8$ | $\eta_{\text{turb}} = 1$ $\eta_{\text{pump}} = 1$ |
|----|--|--|--|--|
| BS | 0.29 | 0.43 | 0.64 | 1.27 |
| IS | 1.18 | 1.20 | 1.23 | 1.27 |

Constants: $L_{\text{filt}} = 10^{-11} \text{ m/s Pa}$, $\mu = 0.000855 \text{ N s/m}^2$.

The transport equation was derived for one fibre neglecting the effect of neighbourhood fibres and the pressure drop of the fresh water flowing outside of the fibre. A real system consists of numerous fibres more or less densely packed together. When the free flowing area of fresh water between the fibres diminishes, i.e. the packing density increases, the pressure loss at the fresh water side increases. Therefore, for densely packed systems the pressure drop could be meaningful even outside the fibre (even though the fresh water flow is diminishing in a pressure-retarded system where the concentrated fluid is inside the lumen). If the pressure losses outside the fibre were significant, the initial hydrostatic pressure at this side should be increased remarkably above the level of the environment. This would affect the permeating flow to increase, but the needed pumping power would increase as well. If one wants to study the effect of different packing densities, the fresh water side should be taken more closely into account in both the transport equation and the net power equation. At this stage the flow arrangement (parallel-flow, counterflow or cross flow) would become meaningful too. So, in practice, the fibres need empty space between each other so that the fresh water could flow between them and thus the power densities of a real system are

somewhat lower than in Table 1, Table 2 and Fig. 11. If, e.g. the flow area of the fresh water between the fibres is equal to the cross-sectional area of the fibres, the power densities will drop to half of the values in Tables 1 and 2 (actually to less than half because the fibre thickness is not accounted).

We studied the system optimizing also the ratio between the net power versus the fibre volume. This is different from the results in Tables 1 and 2, where we first optimized the net power and then divided it by the corresponding volume. This optimizing gave the result that the values of $v_{\text{mean,opt-P}}^0$, $r_{0,\text{opt}}$, $L_{\text{opt-P}}$ should be as small as possible. The same statements about the system dimensions, the losses at inlet and outlet of fibres as mentioned earlier also apply here, so that these kinds of conclusions had to be ruled out within the scope of this work.

5.5. The effect of the filtration coefficient and the dynamic viscosity

The optimal initial hydrostatic pressure difference $\Delta p_{\text{opt-P}}^0$ was found to be independent of L_{filt} and μ but $v_{\text{mean,opt-P}}^0$ and $L_{\text{opt-P}}$ resulted in strong dependency on the L_{filt} and μ (Figs. 13 and 14). The ratio ($P_{\text{maximum}}/A_{\text{fibre surface}}$) remained constant for all values of μ but increased with increasing value of L_{filt} . The volume flow ratio $\dot{V}_0/\Delta\dot{V}$ remained independent of both L_{filt} and μ .

5.6. Minimum entropy generation

The minimization of the entropy production rate (Eq. (39)) of the total osmotic unit results in the initial hydrostatic pressure (Δp^0) being equal to the initial effective osmotic pressure ($\Delta\pi_{\text{eff}}^0$), and both the initial mean velocity (v_{mean}^0) and the fibre length (L) approaching zero. This is a natural result, as in this case all flows will damp i.e. the irreversibilities cease. The unwanted consequence of the ceasing of flows is that the power generation (P) vanishes. Thus, the entropy generation cannot be used in this formula to optimize the system.

Instead, the local rate of entropy generation (σ'''), Eq. (40), results always in a minimum value at some longitudinal non-zero position. An example of this phenomenon is shown in Fig. 15. When started with arbitrary values of v_{mean}^0 and Δp^0 , this optimal position

($L_{\text{opt-}\sigma''}$) was not found to have any dependency on the respective position where power generation results in the maximum value. However, if we calculate the σ''' with initial values of $v_{\text{mean,opt-P}}^0$ and $\Delta p_{\text{opt-P}}^0$, which resulted in optimizing P , the local minimum was always found to settle at a further position than the corresponding value of $L_{\text{opt-P}}$. If both efficiencies η_{turb} and η_{pump} are set as unity, the value of $L_{\text{opt-}\sigma''}$ will settle about 9% further than $L_{\text{opt-P}}$ for both BS and IS. As the efficiency decrease, the corresponding difference increases, for instance, if $\eta_{\text{turb}} = 0.9$ and $\eta_{\text{pump}} = 0.8$, the difference is about 12% for BS and about 30% for IS. The parameters were varied in these calculations between: $\Delta\pi_{\text{eff}}^0$ 5–70 bar, $r_0 = 10$ –250 μm , $L_{\text{filt}} = 10^{-13}$ – 10^{-10} m/s Pa.

5.7. Maximizing the ratio between net power and entropy generation

The maximizing of the function Ψ , the ratio between the net power (P) and the entropy generation rate (σ), does not result in an unequivocal optimal point ($v_{\text{mean,opt}}^0$, Δp_{opt}^0 , L_{opt}) as did the optimization of P . Instead, when the v_{mean}^0 diminishes, the resulting Ψ -value (see Fig. 16(a)) for BS approaches asymptotically the same maximum value for each fibre radius (r_0). The corresponding optimal initial pressure difference ($\Delta p_{\text{opt-}\Psi}^0$) also approaches a consistent value for all fibre radii but the optimal fibre length ($L_{\text{opt-}\Psi}$) remains dependent on the v_{mean}^0 and r_0 (Fig. 16b and c). To obtain net power from the system, the v_{mean}^0 cannot be zero ($v_{\text{mean}}^0 \rightarrow 0 \Rightarrow \Psi \rightarrow \Psi_{\text{max}}$ but $P \rightarrow 0$). Therefore, it is necessary to redefine the optimum of v_{mean}^0 so that $\Psi(v_{\text{mean,opt-}\Psi}^0) \approx \Psi_{\text{max}}$ and $P(v_{\text{mean,opt-}\Psi}^0)$ do not vanish. The new definition we give to the optimal initial mean velocity $v_{\text{mean,opt-}\Psi}^0$ is

$$\frac{\Psi(v_{\text{mean,opt-}\Psi}^0)}{\Psi(v_{\text{mean}}^0 \rightarrow 0)} = 0.99$$

For instance, in the case of Fig. 16, the value of $\Psi(v_{\text{mean}}^0 \rightarrow 0) = 67.73$ K. So, we search the initial mean velocity value for which the function Ψ results in 99% of the value of $\Psi(v_{\text{mean}}^0 \rightarrow 0)$ i.e. for this case $\Psi(v_{\text{mean,opt-}\Psi}^0) = 67.05$ K. Some values of $v_{\text{mean,opt-}\Psi}^0$ are presented in Table 4. In fact, the condition $v_{\text{mean}}^0 \rightarrow 0$ is outside of the validity of this study, as in Section 3.1 we assumed that the diffusion flows in

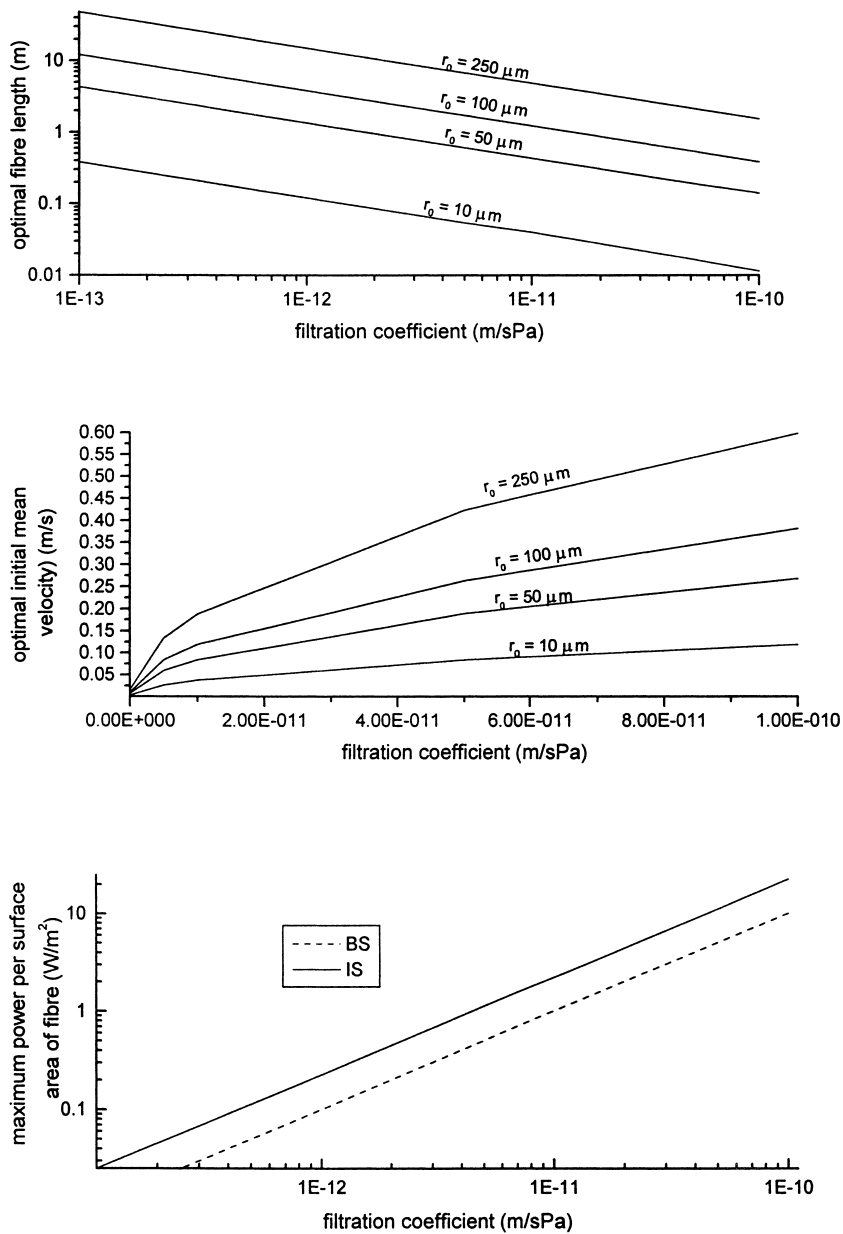


Fig. 13. The effect of the filtration coefficient with different fibre radii on (a) optimal fibre length for the IS; (b) initial mean velocity of brine for the IS; (c) maximum power of the IS. Constant values $\Delta\pi_{\text{eff}} = 20$ bar, $\mu = 8.55 \times 10^{-4}$ N s/m², $\eta_{\text{pump}} = 0.8$ and $\eta_{\text{turb}} = 0.9$ were used.

longitudinal direction are negligible compared to the convective flows. The optimization of IS fails because no maximum value for Ψ in respect to fibre length was found. Instead, Ψ increases rather linearly when the fibre length decreases to even unrealistically small values. The losses at inlet and outlet of the fibre should

be added to the model if the optimizing of Ψ is applied to IS.

When the power densities resulting from the optimization of P and Ψ (Tables 1 and 5) are compared, we find that the optimization of P results in about twice as high values as optimizing Ψ . This was found

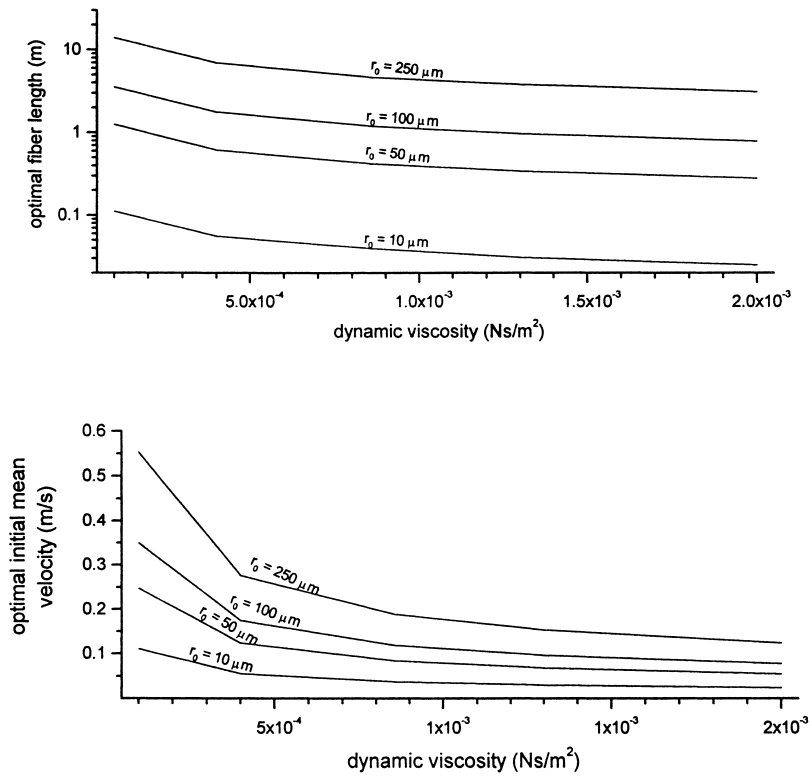


Fig. 14. The effect of dynamic viscosity with different fibre radii on (a) optimum fibre length for the IS and (b) optimum initial mean velocity of brine for the IS. Constant values $\Delta\pi_{\text{eff}} = 20$ bar, $L_{\text{filt}} = 10^{-11}$ m/s Pa, $\eta_{\text{pump}} = 0.8$ and $\eta_{\text{turb}} = 0.9$ were used.

Table 4
Optimal initial mean velocity $v_{\text{mean,opt-}\Psi}^0$ (m/s) for BS

| $\Delta\pi_{\text{eff}}$ (bar) | $r_0 = 10 \mu\text{m}$ | $r_0 = 25 \mu\text{m}$ | $r_0 = 100 \mu\text{m}$ | $r_0 = 250 \mu\text{m}$ |
|--------------------------------|------------------------|------------------------|-------------------------|-------------------------|
| 5 | 0.0005 | 0.0008 | 0.0016 | 0.0025 |
| 20 | 0.0020 | 0.0030 | 0.0063 | 0.010 |
| 40 | 0.0039 | 0.0062 | 0.0125 | 0.020 |
| 70 | 0.0070 | 0.011 | 0.022 | 0.035 |

Parameters: $L_{\text{filt}} = 10^{-11}$ m/s Pa, $\mu = 0.000855$ N s/m², $c_w^0 = 55.55$ kmol/m³, $\gamma = 0.0003/\text{K}$, $\eta_{\text{turb}} = 0.9$, $\eta_{\text{pump}} = 0.8$.

Table 5
Power density (kW/m³) of BS which results in optimizing Ψ

| $\Delta\pi_{\text{eff}}$ (bar) | $r_0 = 10 \mu\text{m}$ | $r_0 = 25 \mu\text{m}$ | $r_0 = 100 \mu\text{m}$ | $r_0 = 250 \mu\text{m}$ |
|--------------------------------|------------------------|------------------------|-------------------------|-------------------------|
| 5 | 6.0 | 2.4 | 0.6 | 0.2 |
| 20 | 98 | 37 | 10 | 3.9 |
| 40 | 391 | 156 | 39 | 16 |
| 70 | 1192 | 474 | 119 | 48 |

Parameters as in Table 4.

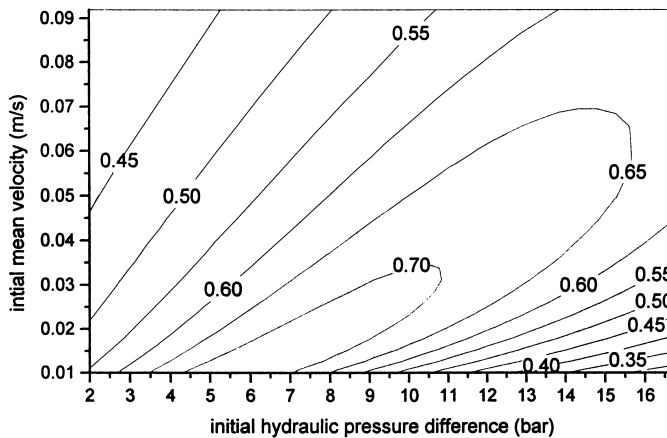
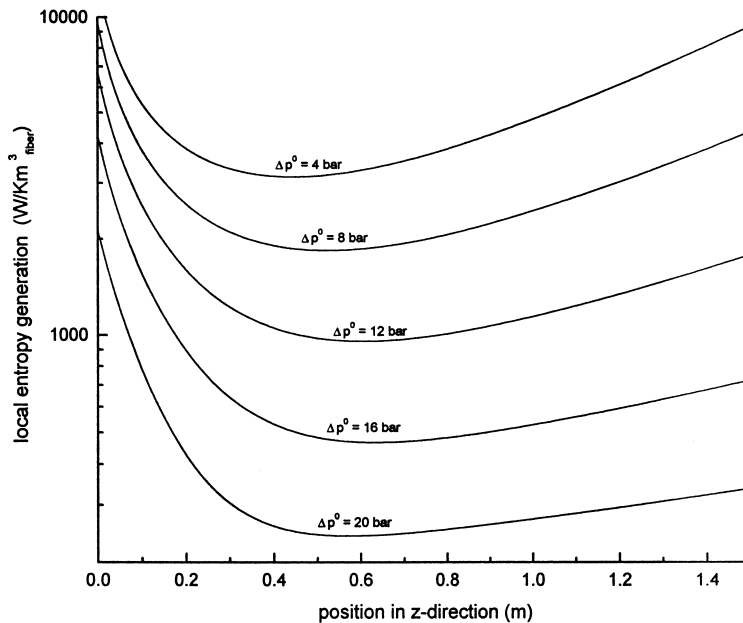


Fig. 15. (a) The local entropy generation (σ''') inside the osmotic unit with $v_{\text{mean}}^0 = 0.08$ m/s; (b) the longitudinal position of fibre ($L_{\text{opt-}\sigma'''}$), in metres, where the local entropy generation is minimum. For both figures: $L_{\text{filt}} = 10^{-11}$ m/s Pa, $\Delta\pi_{\text{eff}}^0 = 25$ bar ($T = 300$ K, $c_s^0 = 1002.3$ mol/m³, $\sigma = 1$), $r_0 = 50$ μm , $\mu = 0.000855$ N s/m², $c_w^0 = 55.55$ kmol/m³, $\gamma = 0.0003/\text{K}$.

to be true for all realistic (achievable today) efficiency of the pump and turbine (Fig. 17). As both the efficiencies approach simultaneously unity, this ratio increases towards infinity and $L_{\text{opt-}\Psi}$ approaches zero. The parameters were varied between $\Delta\pi_{\text{eff}}^0 = 5\text{--}70$ bar, $r_0 = 10\text{--}250$ μm , $L_{\text{filt}} = 10^{-12}$ to 10^{-10} m/sPa, always resulting, with reasonable efficiency,

in about 2.1–2.4 times higher values when P is optimized.

6. Conclusions

The transport equation derived in this study takes into account the effects of dilution and hydrostatic

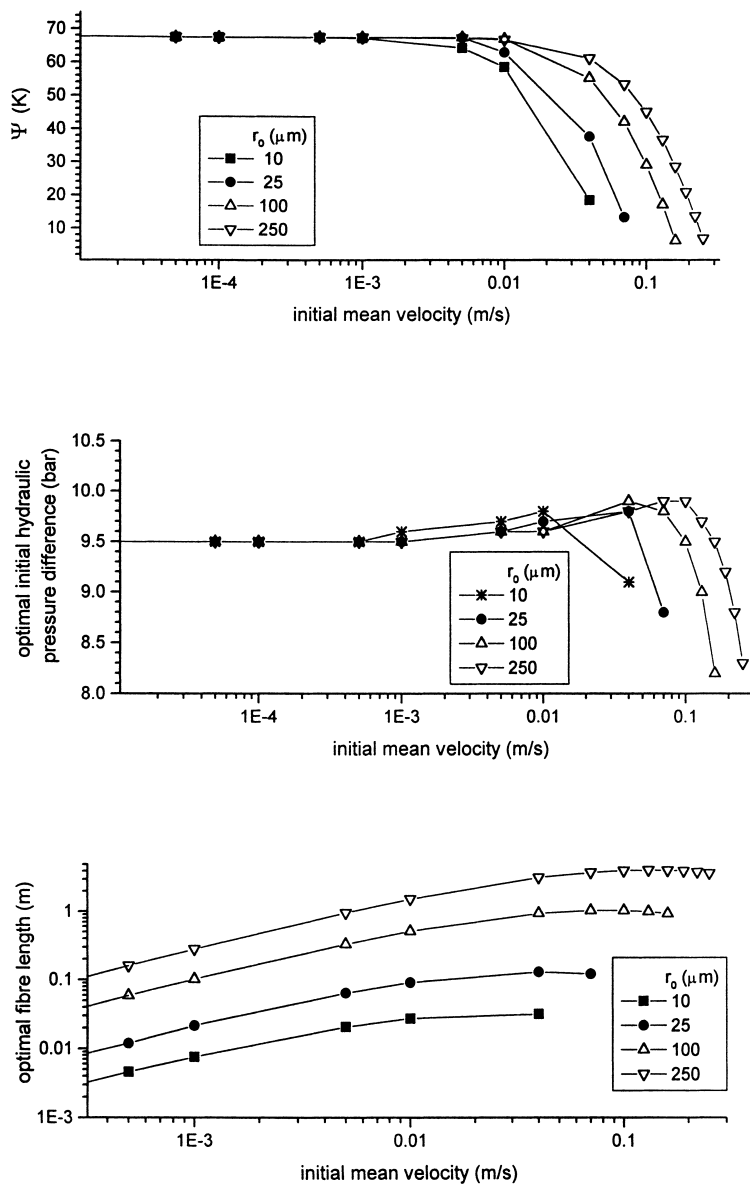


Fig. 16. (a) the ratio between net power and entropy generation; (b) corresponding optimal initial hydrostatic pressure difference; (c) corresponding optimal fibre length. The following constants were used for all figures: $L_{\text{filt}} = 10^{-11}$ m/s Pa, $\Delta\pi_{\text{eff}}^0 = 20$ bar ($T = 300$ K, $c_s^0 = 801.86$ mol/m³, $\sigma = 1$), $\mu = 0.000855$ N s/m², $c_w^0 = 55.55$ kmol/m³, $\gamma = 0.0003$ /K, $\eta_{\text{turb}} = 0.9$, $\eta_{\text{pump}} = 0.8$.

pressure drop of the solution inside the hollow fibre affecting the permeating fresh water flow. The membrane is considered as highly selective i.e. the solute flux through the membrane is assumed to be minimal. Because the equation is derived applying the effective osmotic pressure difference (correction from the

osmotic pressure difference between both sides of an ideal membrane, including the possible internal polarization), small solute fluxes can be accepted as long as the effect of the solute diffusion inside the lumen in radial direction to the concentration boundary layer remains less important than the correspond-

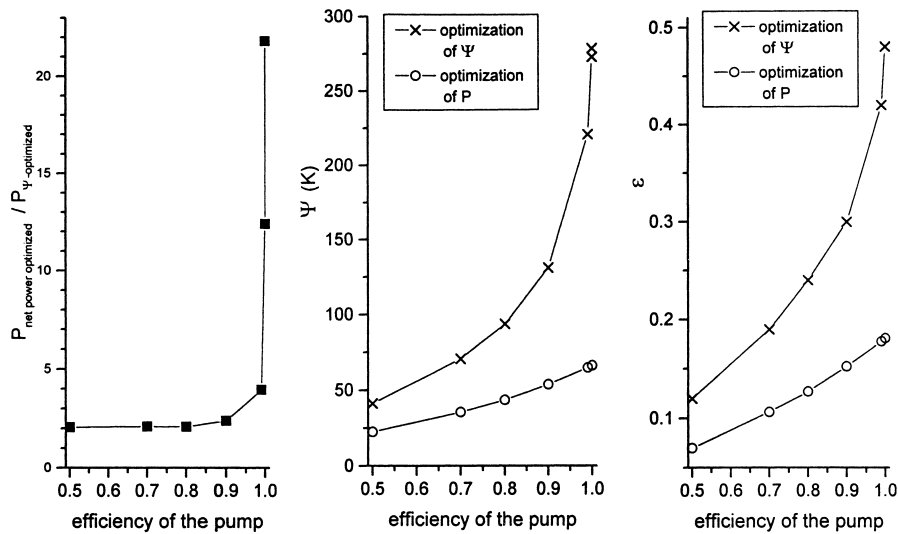


Fig. 17. (a) The ratio between the net powers resulting in optimization of P and Ψ in function of the efficiency of the pump; (b) corresponding behaviour of Ψ ; (c) corresponding behaviour of ϵ (see Eq. (42)). Parameters $L_{\text{filt}} = 10^{-11}$ m/s Pa, $\Delta\pi_{\text{eff}}^0 = 20$ bar ($T = 300$ K, $c_s^0 = 1002.3$ mol/m³, $\sigma = 1$), $r_0 = 25$ μm , $\mu = 0.000855$ N s/m², $c_w^0 = 55.55$ kmol/m³, $\gamma = 0.0003/\text{K}$, $\eta_{\text{turb}} = 0.9$.

ing flow of water. During the derivation of the transport equation, no assumptions of the direction of the permeating flow were made. Thus, the transport equation is applicable to solution flow increasing due to pressure-retarded osmosis or decreasing due to the reverse osmosis as well. Furthermore, direct osmosis can be estimated from the analytical solution which was given in Section 3.1. The pressure drop of the diminishing fresh water flow outside the fibre is neglected. So, the equation should be on its best with loosely packed osmosis permeating systems. Based on the transport equation, the net power function (P) and the entropy generation function (σ) are formed for two different concepts of the pressure-retarded osmosis power generation system. The functions P and Ψ ($=P/\sigma$) are used to optimize the systems.

For a real system to be able to deliver any net power, the initial hydrostatic pressure, the initial velocity and the fibre length should be considered with care. According to this theoretically based study, it is possible not only to localize the positive range of the net power, but also to specify the optimum values for the initial hydrostatic pressure difference between the solution inside the fibre and the fresh water outside the fibre (Δp_{opt}^0), for the initial mean velocity of the solution ($v_{\text{mean,opt}}^0$) and for the fibre length (L_{opt}).

The results show that, when P is maximized, Δp_{opt}^0 can be defined with a good accuracy when the effective osmotic pressure and the pump and turbine efficiencies are given. To define L_{opt} we need to know the inner radius of the fibre, the efficiencies, the membrane and the solution properties, except the osmotic pressure. To determine $v_{\text{mean,opt}}^0$ the inner radius of the fibre and all the membrane and solution properties should be known. The improved system (IS), where the brine is pressurized by recycling it into a tank, was found to result in higher power generation than the basic system (BS). If the physical model of osmotic flow is simplified in such a way that pressure losses and dilution of the solution are neglected, the optimization results remarkably overestimated values for power generation.

The determination of optimum values based on Ψ is more complex. In general, we need all the system and solution parameters. Furthermore, as Ψ was found to approach asymptotically the maximum value when the initial mean velocity decreases ($v_{\text{mean}}^0 \rightarrow 0 \Rightarrow \Psi \rightarrow \Psi_{\text{max}}$ but $P \rightarrow 0$), we had to redefine the definition of $v_{\text{mean,opt}}^0$. The optimal values resulting from these two methods differ, sometimes considerably, from each other. When Ψ was maximized, the net power density (net power per fibre volume) of BS always dropped to less than half of the maximum power density. On the

other hand, the optimization of P drops remarkably the values of Ψ from its maximum values.

The local entropy generation always resulted in a minimum value at a certain longitudinal position inside the fibre. This minimum position settles further than the corresponding optimal position resulting from the optimization of P .

7. Nomenclature

| | |
|------------------------|--|
| A | surface area, m ² |
| A_1, A_2, A_3, \dots | constants |
| C | concentration, mol/m ³ |
| d | total differential |
| D | diffusion coefficient, m ² /s |
| $f(r)$ | function that describes the dependence of salt concentration on radial direction |
| $F(r)$ | function that describes the dependence of z -component of mass average velocity flow on radial direction |
| $g(z)$ | function that describes the dependence of salt concentration on longitudinal direction |
| $G(z)$ | function that describes the dependence of z -component of mass average velocity flow on longitudinal direction |
| h | molar specific enthalpy, J/mol |
| \mathbf{j} | diffusion flux, kg/m ² s |
| L | length of a fibre, m |
| L_{filt} | filtration coefficient, m/s Pa |
| L_{refl} | reflection coefficient (interpreted so that it takes into account also the internal polarization), non dimensional |
| \mathbf{n} | mass flow relative to stationary coordinates, kg/m ² s |
| N | molar flow, mol/s |
| p | hydrostatic pressure, bar or Pa in equations |
| p_{loss} | hydrostatic pressure losses of the brine, bar |
| P | power, W |
| \dot{Q} | heat flux, W |
| r_0 | fibre radius, μm , or m in equations |
| s | molar specific entropy, J/mol K |

| | |
|---------------|---|
| S | entropy, J/K |
| R | universal gas constant, J/mol K |
| T | temperature, K |
| \mathbf{v} | mass average velocity vector, m/s |
| v | partial molar volume, m ³ /mol |
| \dot{V} | volume flow, m ³ /s |
| v | Mass average velocity, m/s |
| x | mole fraction |
| ε | energy conversion efficiency (defined in Eq. (42)) |
| Δ | difference |
| ∂ | partial differential |
| η | efficiency |
| σ | rate of entropy generation, W/K |
| σ''' | local rate of entropy generation, W/m ³ K |
| μ | dynamic viscosity, N s/m ² |
| ρ | total density of a solution, kg/m ³ |
| ρ_s | partial density of salt, kg/m ³ |
| ∇ | gradient |
| Ψ | ratio between net power and entropy generation, K (defined in Eq. (41)) |
| π | osmotic pressure. bar or Pa in equations or 3.14159... |
| γ | isobaric coefficient of volume expansion, 1/K |

Indexes

| | |
|-------------|---|
| BS | basic system |
| fw | fresh water |
| i | species |
| IS | improved system |
| mean | mean value over the cross-sectional area of the fibre |
| n | iteration number |
| opt | optimal value |
| opt- P | optimal value when net power (P) is optimized |
| opt- Ψ | optimal value when the ratio (Ψ) between net power and entropy generation is optimized |
| perm | permeating |
| r | radial direction |
| ref | reference |
| s | salt |
| turb | turbine |
| w | water in a solution |

z longitudinal direction
 0 initial value i.e. value at the entrance
 of the osmotic unit

References

- [1] S. Loeb, Production of energy from concentrated brine by pressure-retarded osmosis, *J. Membr. Sci.* 1 (1976) 49–63.
- [2] S. Loeb, G.D. Mehta, A two-coefficient water transport equation for pressure-retarded osmosis, *J. Membr. Sci.* 4 (1979) 351–362.
- [3] G.D. Wick, Power from salinity gradients, *Energy* 3 (1978) 95–100.
- [4] G.D. Mehta, S. Loeb, Internal polarization in the porous substructures of a semi-permeable membrane under pressure-retarded osmosis, *J. Membr. Sci.* 4 (1978) 261–265.
- [5] K.L. Lee, R.W. Baker, H.K. Lonsdale, Membranes for power generation by pressure-retarded osmosis, *J. Membr. Sci.* 8 (1981) 141–171.
- [6] S. Loeb, T. Honda, M. Reali, Comparative mechanical efficiency of several plant configurations using a pressure-retarded osmosis energy converter, *J. Membr. Sci.* 51 (1990) 323–335.
- [7] A. Katchalsky, P.F. Curran, *Non-equilibrium Thermodynamics in Biophysics*, Harvard University Press, Cambridge, 1965.
- [8] S. Loeb, L. Titelman, E. Korngold, J. Freiman, Effect of porous support fabric on osmosis through a Loeb–Sourirajan type asymmetric membrane, *J. Membr. Sci.* 129 (1997) 243–249.